

# Multimodal Trajectory Representation Learning for Travel Time Estimation

Zhi Liu

Zhejiang University of Technology  
Hangzhou, China  
lzhi@zjut.edu.cn

Zhehao Dai

Zhejiang University of Technology  
Hangzhou, China  
zhehaodai@outlook.com

Xuyuan Hu

Zhejiang University of Technology  
Hangzhou, China  
huxvyuan@gmail.com

Xiao Han\*

Zhejiang University of Technology  
Hangzhou, China  
hahahenha@gmail.com

Zhaolin Deng

Zhejiang University of Technology  
Hangzhou, China  
211123120032@zjut.edu.cn

Guojiang Shen

Zhejiang University of Technology  
Hangzhou, China  
guojiangshen1975@zjut.edu.cn

Xiangjie Kong

Zhejiang University of Technology  
Hangzhou, China  
xjkong@ieee.org

## Abstract

Accurate travel time estimation (TTE) plays a crucial role in intelligent transportation systems. However, it remains challenging due to heterogeneous data sources and complex traffic dynamics. Moreover, conventional approaches typically convert trajectories into fixed-length representations, neglecting the inherent variability of real-world trajectories, which often leads to information loss or feature redundancy. To address these challenges, this paper introduces the Multimodal Dynamic Trajectory Integration (MDTI) framework—a novel multimodal trajectory representation learning approach that integrates GPS sequences, grid trajectories, and road network constraints to enhance TTE accuracy. MDTI employs modality-specific encoders and a cross-modal interaction module to capture complementary spatial, temporal, and topological semantics, while a dynamic trajectory modeling mechanism adaptively regulates information density for trajectories of varying lengths. Two self-supervised pretraining objectives, named contrastive alignment and masked language modeling, further strengthen multimodal consistency and contextual understanding. Extensive experiments on three real-world datasets demonstrate that MDTI consistently outperforms state-of-the-art baselines, confirming its robustness and strong generalization abilities. The code is publicly available at: <https://github.com/freshhxy/MDTI/>

**Relevance Statement:** This paper proposes a method to integrate open-source GPS sensor data, grid trajectories, and road network semantics for dynamic multimodal trajectory representation learning, addressing semantic fusion and representation challenges in large-scale mobility data on the web.

Permission to make digital or hard copies of all or part of this work for personal or classroom use is granted without fee provided that copies are not made or distributed for profit or commercial advantage and that copies bear this notice and the full citation on the first page. Copyrights for components of this work owned by others than the author(s) must be honored. Abstracting with credit is permitted. To copy otherwise, or republish, to post on servers or to redistribute to lists, requires prior specific permission and/or a fee. Request permissions from [permissions@acm.org](mailto:permissions@acm.org).

Conference'XX, Washington, DC, USA

© 2026 Copyright held by the owner/author(s). Publication rights licensed to ACM.  
ACM ISBN 978-1-4503-XXXX-X/2018/06

## CCS Concepts

- Information systems → Spatial-temporal systems; • Computing methodologies → Artificial intelligence.

## Keywords

Trajectory representation learning, Multimodal data mining

## ACM Reference Format:

Zhi Liu, Xuyuan Hu, Xiao Han\*, Zhehao Dai, Zhaolin Deng, Guojiang Shen, and Xiangjie Kong. 2026. Multimodal Trajectory Representation Learning for Travel Time Estimation. In . ACM, New York, NY, USA, 11 pages.

## 1 Introduction

With the rapid development of connected vehicle technologies, vast amounts of trajectory-based sensor data are continuously generated and shared on the Web. Within this context, travel time estimation (TTE) [8] has emerged as a core task in traffic flow analysis. By transforming heterogeneous trajectory data into a unified indicator, TTE provides essential input for downstream decision-making processes such as route planning, traffic guidance, and system-wide control. TTE focuses on predicting the time required to traverse a specific route from an origin to a destination, while accounting for dynamic factors such as traffic conditions, road characteristics, and environmental influences [16]. Accurate predictions enable more efficient route planning, congestion mitigation, and resource management in urban transportation systems. Core aspects of TTE include its dependence on real-time data, integration of multimodal traffic information, and adaptability to rapidly changing traffic patterns. The main challenge, however, lies in effectively modeling the inherent complexity of multimodal spatiotemporal traffic systems. This underscores the need for advanced approaches to improve the precision and robustness of TTE.

Trajectory representation learning [12, 31] provides an effective framework for modeling multimodal spatiotemporal data, playing a crucial role in reconstructing complex trajectory patterns and supporting TTE tasks. Early trajectory representation learning (TRL)

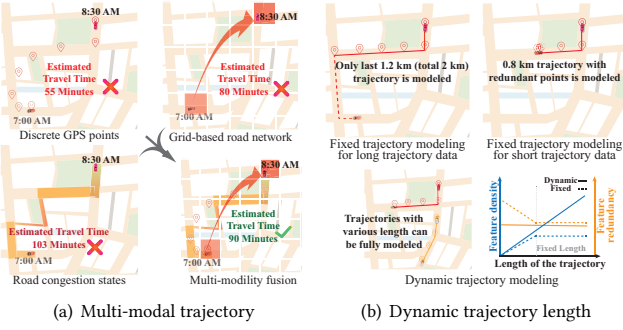


Figure 1: Toy examples of trajectory data.

approaches mainly employed univariate sequence-to-sequence architectures [9, 24] to encode raw GPS trajectories [7, 12, 31]. In these methods, trajectories are modeled as sequences of time-stamped data points, where each point corresponds to a single variable such as latitude, longitude, or speed. Although such models effectively capture temporal dependencies and map sequential data into latent embeddings, they fall short in representing multimodal trajectory information, thereby limiting their applicability and robustness in real-world traffic scenarios.

As illustrated in Figure 1(a), discrete GPS trajectory data often suffers from drift (top left), grid-based road network modeling leads to limited accuracy (top right), and congestion-based analysis depends heavily on real-time updates (bottom left). Consequently, relying on a single-source trajectory data representation is insufficient for accurate and reliable travel time estimation. In contrast, integrating multiple information sources within a unified framework enables more precise and robust prediction of vehicle travel times, as demonstrated in the bottom right of Figure 1(a). Therefore, extracting semantic structures from different modalities and achieving effective alignment and fusion is a major challenge.

Another challenge in trajectory representation lies in converting dynamically varying trajectory samples into fixed-length feature vectors. For instance, GPS data collected from different vehicles often differ in spatiotemporal sampling frequencies [1], sequence lengths [27], and other factors. However, many existing methods address trajectory variability by setting a maximum sequence length [10], padding shorter trajectories with zeros, and clipping longer ones for representation learning. However, these strategies often introduce redundant noise or cause information loss. As shown in Figure 1(b), when trajectories exceed the maximum threshold (top left), only the last segment is retained, preventing a full representation of the overall trajectory. Conversely, shorter trajectories (top right) are padded with redundant GPS points, which overemphasize local features such as the starting point and hinder effective representation learning. To overcome these issues, dynamic modeling techniques (bottom) can adaptively generate embeddings with differentiated information density and reduced redundancy as trajectory lengths vary. Therefore, the second challenge addressed in this work is to incorporate dynamic modeling into trajectory representation learning, ensuring fixed-length embeddings that better capture essential spatiotemporal patterns.

To address these challenges, we propose the Multimodal Dynamic Trajectory Integration Model (MDTI), which jointly models GPS sequences, grid trajectories, and road network constraints to comprehensively represent trajectory features for travel time estimation. The proposed framework incorporates a cross-modal interaction module that captures relationships among different modalities, enabling effective alignment and consistent semantic extraction. In addition, dedicated modality-specific encoders map heterogeneous inputs into a unified feature space, facilitating seamless multimodal fusion. Furthermore, a dynamic trajectory extraction module adaptively adjusts the information density of trajectory feature vectors according to trajectory length, preventing feature over-concentration in local embeddings and promoting balanced and discriminative representations. The main contributions of this work are summarized as follows:

- We propose the MDTI framework, which jointly leverages GPS sequences, grid trajectories, and road network constraints to systematically overcome the limitations of existing methods that rely on single or dual modalities, thereby enhancing semantic richness and completeness in trajectory representation.
- We design a cross-modal interaction module and a dynamic trajectory modeling module: the former aligns heterogeneous features and extracts consistent semantics across modalities, while the latter adaptively encodes trajectories of varying lengths, mitigating the information loss and redundancy inherent in fixed-length modeling.
- Extensive experiments on multiple real-world transportation datasets demonstrate that MDTI significantly outperforms state-of-the-art methods in TTE, validating the effectiveness of multimodal fusion and dynamic modeling in addressing the core challenges of trajectory representation.

## 2 Related Work

### 2.1 Multimodal Trajectory Representation Learning

TRL encodes sequences of states, actions, or spatiotemporal points into compact vectors that preserve temporal structures and semantic information. Early work introduced Traj2vec [31], which directly modeled raw GPS trajectories as point sequences to derive compact representations for downstream tasks. However, due to inherent issues in GPS data—such as positioning drift, U-turns, and redundant sampling—these approaches often produced unstable and poorly transferable representations.

To overcome these limitations, grid-based trajectory modeling methods have been proposed [3, 13, 30]. By discretizing the spatial domain into grid cells and constructing graph-based structures, these approaches enhance the capacity for semantic and structural trajectory modeling. For instance, t2vec [13] employs an encoder-decoder architecture [23] to learn robust trajectory representations from noisy or low-quality data. E2DTC [6] introduces a self-training mechanism to capture latent spatial dependencies within grid-based embeddings. More recently, TrajCL [3] adopts contrastive learning to jointly model spatial correlations and structural relationships among trajectories.

In parallel, road-based trajectory modeling has emerged as another major direction. Using map-matching techniques [17, 29],

trajectories are aligned with road networks, which introduces topological constraints and enables richer representations of travel patterns. JCLRNT [20] generates contrastive samples between roads by leveraging contextual neighbors and constructing trajectory-level contrasts through detour path replacement. Start [10] incorporates temporal regularities and travel semantics into a self-supervised framework, improving both representation quality and generalization. JGRM [18] further strengthens spatiotemporal road features by mapping raw GPS points to corresponding road segments. Building on this trend, GREEN [33] integrates grid-based and road-based representations, exploiting their complementarity to yield more comprehensive trajectory embeddings and improved downstream task performance. Building on these advances, our study takes a further step by integrating GPS-based, grid-based, and road-based information into a unified multimodal framework, thereby addressing the limitations of single-modality representations for TTE.

## 2.2 Travel Time Estimation

TTE refers to predicting the time required to traverse a route or road segment from origin to destination. Existing studies can be broadly categorized into path-based methods and origin–destination (OD)-based methods.

Path-based methods use complete trajectories or trajectory segments as input, enabling the modeling of vehicle dynamics within the road network. These approaches typically leverage road segment features, trajectory sequences, or path structures to capture spatiotemporal dependencies. For instance, DeepTTE [26] integrates graph convolutional networks with LSTM [32] to model the spatiotemporal dependencies of GPS sequences. HierETA [4] introduces a multi-view hierarchical choice model for fine-grained and interpretable TTE. MultTTE [15] jointly models trajectory, attribute, and semantic sequences, and further applies self-supervised learning to improve generalization, yielding significant gains in prediction accuracy.

OD-based methods, by contrast, rely only on origin–destination pairs and departure times, avoiding the need for full trajectory inputs. TEMP [28] estimates travel times using only OD pairs and departure information. Extending this, MURAT [14] incorporates road network structures and driver behavior to enrich spatiotemporal embeddings. More recently, DutyTTE [19] combines reinforcement learning with a mixture-of-experts framework to optimize path prediction and capture segment-level uncertainty, enabling confidence interval estimation.

Building on these directions, our work is more closely aligned with path-based approaches, as it exploits the spatiotemporal information embedded in complete trajectories to achieve more accurate and robust TTE.

## 3 Overview

### 3.1 Definitions

**Definition 1 (GPS Trajectory).** A GPS trajectory is defined as an ordered sequence of raw GPS points collected at a fixed sampling interval by a GPS-enabled device:

$$\mathcal{T}^{gps} = \{p_i\}_{i=1}^T, \quad p_i = (x_i, y_i, t_i), \quad (1)$$

where  $x_i$  and  $y_i$  denote longitude and latitude, and  $t_i$  denotes the timestamp. Here,  $T$  is the total number of points in the trajectory.

**Definition 2 (Grid Trajectory).** A grid trajectory  $\mathcal{T}^{grid}$  maps GPS points onto a discretized spatial grid. Let the region of interest be partitioned into  $M \times N$  cells, each representing a spatial unit. The trajectory is then expressed as a sequence of grid cell identifiers:

$$\mathcal{T}^{grid} = \{g_t\}_{t=1}^T, \quad g_t \in \{1, \dots, M \times N\},$$

where  $g_t$  denotes the identifier (ID) of the grid cell visited at time  $t$ .

**Definition 3 (Road Network).** A road network is represented as a directed graph  $\mathcal{G} = (\mathcal{V}, \mathcal{E})$ , where  $\mathcal{V} = \{v_1, v_2, \dots, v_{|\mathcal{V}|}\}$  denotes the set of vertices, and each vertex  $v_i \in \mathcal{V}$  corresponds to a distinct road segment.  $\mathcal{E} \subseteq \mathcal{V} \times \mathcal{V}$  denotes the set of directed edges, where each edge  $e_{ij} = (v_i, v_j) \in \mathcal{E}$  represents the navigable connection from road segment  $v_i$  to  $v_j$ .

**Definition 4 (Road Trajectory).** A road trajectory  $\mathcal{T}^{road}$  is a timestamped sequence of road segments obtained by map-matching GPS points  $\mathcal{T}^{gps}$  to the road network  $\mathcal{G}$ . It can be expressed as

$$\mathcal{T}^{road} = \{v_t\}_{t=1}^T, \quad v_t \in \mathcal{V},$$

where  $v_t$  denotes the road segment visited at time  $t$ .

## 4 Methodology

In this section, we present the proposed MDTI framework in detail. The overall architecture is shown in Figure 2. To handle multimodal trajectory data, three dedicated encoders—Grid Encoder, GPS Encoder, and Road Encoder—are designed, providing the model with preliminary multimodal processing capability. Specifically, graph attention and graph neural networks are employed to encode map-matched road trajectories, while large-model semantic analysis enhances the representation of raw GPS data. A multimodal fusion module is then introduced to align and integrate information across modalities, producing unified embeddings for TTE. In addition, we propose a dynamic trajectory alignment module that adaptively enriches the information density of embeddings, reducing redundancy and improving the accuracy of downstream TTE tasks. Finally, two complementary loss functions are applied to stabilize training and optimize performance. The following subsections provide a detailed description of each module in the MDTI framework.

### 4.1 Grid Encoder

Conventional grid-based modeling represents each cell and its internal trajectory points only by cell IDs, leading to sparse representations and limited adjacency awareness. To address this, we introduce a graph attention network (GAT)-based [25] embedding module that dynamically computes cell embeddings using input features such as speed and time. An 8-neighborhood connectivity scheme is adopted to better capture local spatial dependencies among grid cells.

Directly modeling a city-scale trajectory graph is computationally prohibitive. We therefore adopt a local subgraph strategy: for each trajectory point, we build a  $3 \times 3$  grid-centered subgraph consisting of the current cell and its eight neighbors. This leverages the spatial locality of vehicle motion—single-step transitions rarely extend beyond adjacent cells—so the local neighborhood suffices to capture short-range dependencies while preserving trajectory continuity. Formally, for each node  $i$ , we retain edges only to itself

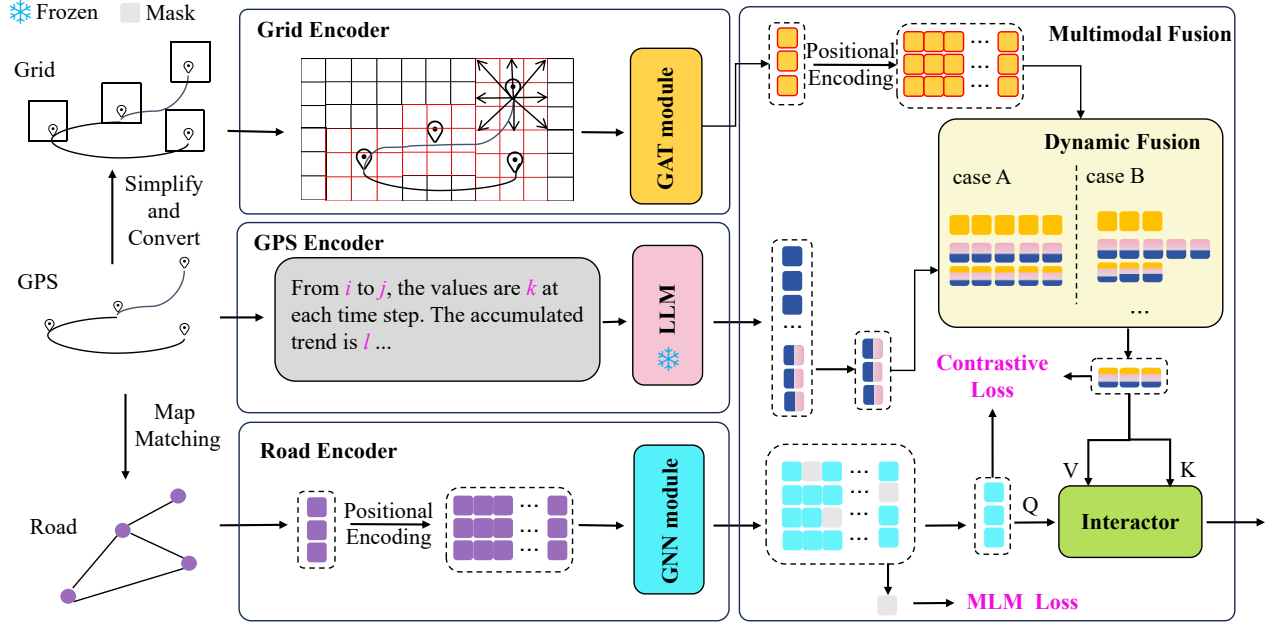


**Figure 2: Overall architecture of the proposed MDTI framework.**

and its eight immediate neighbors, yielding a first-order adjacency matrix  $A$ :

$$A_{ij} = \begin{cases} 1, & j = i \text{ or } j \in \mathcal{N}(i), \\ 0, & \text{otherwise.} \end{cases} \quad (2)$$

Here,  $\mathcal{N}(i)$  denotes the 8-neighborhood of node  $i$ . This localized construction prevents the introduction of long-range, irrelevant edges and ensures that trajectory modeling relies primarily on adjacent regions.

Given the graph structure  $\mathcal{G}_{\text{grid}} = (X, A)$ , each grid cell is treated as a node, with its channel vector serving as the initial node feature. Based on the adjacency matrix  $A$ , nodes are connected to their direct neighbors to form the local subgraph.

To capture spatial dependencies, the node features are encoded using a two-layer GAT. The GAT iteratively aggregates information from neighboring nodes according to the attention mechanism. For the  $l$ -th GAT layer, the embedding of node  $i$  is updated as:

$$h_i^{(l+1)} = \sigma \left( \sum_{j \in \mathcal{N}(i) \cup \{i\}} \alpha_{ij}^{(l)} W^{(l)} h_j^{(l)} \right), \quad (3)$$

where  $h_i^{(l)}$  is the embedding of node  $i$  at layer  $l$ ,  $W^{(l)}$  is the learnable weight matrix,  $\alpha_{ij}^{(l)}$  is the attention coefficient between nodes  $i$  and  $j$ , and  $\sigma(\cdot)$  is a nonlinear activation function.

The attention coefficients are computed as:

$$\alpha_{ij}^{(l)} = \frac{\exp \left( \text{LeakyReLU} \left( a^\top \left[ W^{(l)} h_i^{(l)} \parallel W^{(l)} h_j^{(l)} \right] \right) \right)}{\sum_{k \in \mathcal{N}(i) \cup \{i\}} \exp \left( \text{LeakyReLU} \left( a^\top \left[ W^{(l)} h_i^{(l)} \parallel W^{(l)} h_k^{(l)} \right] \right) \right)}, \quad (4)$$

where  $a$  is the learnable attention vector and  $\parallel$  denotes vector concatenation.

After two successive GAT layers, the node embeddings are aggregated into

$$H^{(2)} = \sigma \left( \text{GATConv}^{(2)} \left( \sigma \left( \text{GATConv}^{(1)} \left( X, A \right) \right), A \right) \right), \quad (5)$$

and we define  $H = H^{(2)}$  as the final grid-level representation. Before applying the projection, we aggregate the node embeddings of all grid cells into the matrix form  $H$ , which serves as the grid-level embedding map for subsequent temporal modeling. The embedding sequence is then projected as

$$G_{\text{emb}} = \text{Proj}(H) \in \mathbb{R}^{T \times D}, \quad (6)$$

where  $\text{Proj}(\cdot)$  denotes a linear projection,  $T$  is the number of temporal segments, and  $D$  is the embedding dimension of the Transformer input. The resulting representation  $G_{\text{emb}} = \{G_0, G_1, \dots, G_T\}$  serves as the spatio-temporal embedding sequence of grid nodes, with  $G_0$  corresponding to the [CLS] token, and the remaining tokens representing different time segments of the trajectory are mapped onto the spatial grids. This sequence embedding is then used as input for subsequent trajectory sequence modeling and Transformer-based encoding.

## 4.2 GPS Encoder

GPS data often exhibit spatiotemporal inconsistencies, including variations in timestamps, geographical locations, and sampling frequencies across trajectories. This heterogeneity poses major challenges for TTE, as conventional models struggle to capture inter-trajectory similarities and critical movement patterns from non-uniformly sampled data, resulting in reduced prediction accuracy. To address this issue, we explore the use of large language models (LLMs), leveraging their strong sequence modeling capabilities. However, applying LLMs directly to raw spatiotemporal trajectories faces a key obstacle: a modality gap between continuous coordinate values and the discrete token structure expected by LLMs, compounded by the absence of explicit semantic structure in raw GPS data. To bridge this gap, we propose a dedicated spatial discretization encoding method that maps continuous spatiotemporal coordinates into a sequence of discrete tokens.

Specifically, we decompose each trajectory into a sequence of structured textual segments with explicit semantics. Each trajectory is represented as a sequence of  $T$  time steps, where each time step consists of three numerical channels, corresponding to the longitude, latitude, and temporal feature (e.g., timestamp or velocity). These channels jointly describe the spatiotemporal state of the moving object at each sampling point, serving as the fundamental input for local motion feature extraction. To extract local motion features, we divide the trajectory into non-overlapping chunks of length three, producing a set of sub-trajectories  $\{\mathcal{S}_m\}_{m=1}^{T/3}$ . The choice of length three is based on empirical observations [22]: it is long enough to capture local motion patterns while remaining computationally efficient for large-scale datasets. Each sub-trajectory  $\mathcal{S}_m$  is flattened into a 9-dimensional vector  $\tilde{p}_m$ . To capture representative spatial-temporal motion patterns, we compare each  $\tilde{p}_m$  with a pattern library  $P = \{P_k\}_{k=1}^K \in \mathbb{R}^{K \times 9}$ , where  $K$  denotes the number of predefined reference patterns. The similarity between  $\tilde{p}_m$  and  $P_k$  is computed as:

$$S_{m,k} = \exp\left(-\frac{\|\tilde{p}_m - P_k\|_2}{2\sqrt{3}}\right). \quad (7)$$

The formula converts the similarities between each sub-trajectory and the prototypes into comparable weights by exponentiating the Euclidean distances, thereby identifying the most representative motion patterns. To further enhance semantic expressiveness, we also extract cumulative trend quantities from the original sequence:

$$\Delta = \sum_{t=2}^T (v_t - v_{t-1}), \quad (8)$$

where  $v_t$  represents the observed motion value at timestamp  $t$ .

After obtaining the structured motion information, we construct a natural-language prompt that integrates the temporal indices, cumulative trend, and pattern similarity results from Equation 8. The prompt for the  $i$ -th trajectory segment is formulated as:

$$\text{Prompt}_i = f(\text{index}, \text{values}, \Delta, \text{patterns}, S_{i,k}), \quad (9)$$

where  $f(\cdot)$  denotes the textual formatting function that converts numerical features into natural-language sentences. After feeding the prompts into a pre-trained language model, we take the embedding of the final token as the semantic representation of the current

segment. Specifically, the embedding of the last token from the language model  $\text{LM}(\cdot)$  output serves as the representation vector for the segment:

$$z_i = \text{LastToken}(\text{LM}(\text{Prompt})) \in \mathbb{R}^{d_{\text{LM}}}. \quad (10)$$

By aggregating all entities in a batch, we obtain the GPS modality representation:

$$Z = \{z_1, z_2, \dots, z_N\}, \quad (11)$$

which captures the real motion patterns of the vehicle in continuous space.

## 4.3 Dynamic FusionAlign

Traditional cross-attention fusion mechanisms enable interaction between modalities but suffer from inherent asymmetry: one modality dominates as the query source while the other serves as the key-value counterpart, leading to imbalanced fusion and difficulty adapting to varying sequence lengths and structures. To address this, we propose a dynamic fusion mechanism that replaces the dominant–subordinate paradigm with symmetric and adaptive deep fusion, allowing bidirectional feature enhancement through fine-grained alignment and maximizing complementary information integration. In our framework, the trajectory representation generated by the GPS encoder acts as a prompt that guides and reinforces sequence learning in the grid encoder. Unlike conventional methods that simply concatenate or append GPS features to downstream predictors, our Dynamic Fusion module operates within the encoding stage, establishing early cross-modal correspondences between grid-based and GPS-based representations to ensure temporal and spatial consistency across modalities.

To guarantee that the two modalities can be effectively fused, we first apply a linear projection that maps GPS embeddings into the same latent space as the grid encoder output:

$$z'_t = \text{Proj}(z_t), \quad t = 1, \dots, T. \quad (12)$$

At the level of length, we introduce an alignment strategy to ensure consistent mapping between GPS sequences and grid tokens. When the GPS sequence is longer than the grid sequence, redundant temporal information is removed through truncation; when it is shorter, a zero-padding strategy is applied to preserve one-to-one correspondence. This mechanism achieves precise timestep synchronization across modalities and guarantees temporal consistency between GPS cues and grid tokens, providing a solid representation basis for subsequent fusion.

Finally, the aligned GPS sequence  $e'$  is injected into the grid sequence via a residual fusion mechanism:

$$\tilde{G}_t = G_t + z'_t, \quad t = 1, \dots, T, \quad (13)$$

where  $\tilde{G}_t$  denotes the fused representation. This design preserves the spatial modeling capacity of the grid encoder while explicitly incorporating GPS prompts, thereby improving the consistency and alignment of the learned representations.

## 4.4 Road Encoder

The road modality provides topological constraints from the underlying road network, which are essential for TRL. Unlike GPS

points that directly capture continuous spatio-temporal observations, road sequences are naturally embedded in a graph structure, where adjacency and accessibility are governed by the topology. To effectively capture such structured dependencies, we adopt a hybrid design: a GAT on the graph side to update road node embeddings, and a Transformer encoder on the sequence side to model temporal dependencies within trajectories.

On the graph side, each road node feature  $h_i$  is first projected into a unified embedding space through a linear transformation and then updated using stacked GATConv layers. The update process follows the same attention-based aggregation formulation as defined in Section 4.1 (Eq. 3–4).

Unlike the grid encoder, where the neighborhood  $\mathcal{N}(i)$  is defined by fixed spatial proximity in a  $3 \times 3$  grid, the road encoder constructs  $\mathcal{N}(i)$  according to the topological connectivity of the road network. This allows message passing along physically connected road segments rather than adjacent spatial grids. Through this topology-aware aggregation, each node representation integrates its own attributes and the structural dependencies of neighboring roads, producing road-aware graph embeddings  $g_{emb}$ .

On the sequence side, we construct the road sequence embedding table by augmenting  $\mathbf{R}_{emb}$  with three special tokens [PAD], [CLS], and [MASK]. Given a trajectory  $\mathbf{R}_{traj}$ , we obtain the corresponding sequence embeddings and further add temporal embeddings (week index and minute index), type embeddings, and positional encodings  $PE(\cdot)$  to preserve ordering. A padding mask ensures that attention is only applied to valid road segments.

The sequence encoder consists of stacked Transformer layers. In each layer, self-attention is first performed on the type embeddings, producing attention scores that are treated as adaptive priors  $B$ . These priors are then injected into the main self-attention computation:

$$\text{Attn}(Q, K, V) = \text{Softmax}\left(\frac{QK^\top}{\sqrt{d_k}} + B\right)V, \quad (14)$$

which explicitly incorporates structural priors into the trajectory modeling process. After multiple layers, the output sequence representations are projected into a shared space, and the first [CLS] token is taken as the trajectory-level representation. Finally, we denote the encoded road sequence representation as

$$\mathbf{R} = \{\mathbf{R}_t\}_{t=1}^T, \quad (15)$$

where  $\mathbf{R}_t$  represents the contextualized embedding of the  $t$ -th road segment after GAT-based graph encoding and Transformer modeling. The overall trajectory-level representation is derived from the [CLS] token of  $\mathbf{R}$ .

## 4.5 Multimodal Interactor

A central challenge in spatiotemporal modeling lies in the effective fusion of heterogeneous modalities, such as GPS-based trajectory sequences and grid-based spatial features. Traditional fusion approaches (e.g., cross-attention [24]) often fail to establish fine-grained spatiotemporal correspondences, which is particularly detrimental for TTE. To overcome this, we design a modality interaction mechanism that leverages multi-head cross-attention to explicitly capture inter-modal dependencies, thereby mitigating sequence-length and sampling-frequency mismatches and achieving fine-grained semantic alignment across modalities.

Specifically, given a road sequence  $X \in \mathbb{R}^{B \times L_x \times d}$  and a dynamically fused grid representation  $M \in \mathbb{R}^{B \times L_y \times d}$ , we compute the cross-modal attention as:

$$\text{Attn}(X, M) = \text{Softmax}\left(\frac{(XW_Q)(MW_K)^\top}{\sqrt{d_k}} + M_s\right)(MW_V), \quad (16)$$

where  $W_Q, W_K, W_V \in \mathbb{R}^{d \times d_k}$  are learnable projection matrices, and  $M_s$  denotes the spatial alignment bias. In this design, the road sequence  $X$  acts as the *query*, actively retrieving relevant contextual information, while the fused grid representation  $M$  serves as the *key* and *value*, providing rich spatial semantics. This formulation enables adaptive and context-aware feature interaction between modalities, guided by the trajectory structure.

The fused output is then refined through a residual connection followed by a feed-forward network (FFN):

$$\hat{X} = \text{FFN}(X + \text{Attn}(X, M)), \quad (17)$$

where  $\hat{X}$  denotes the final fused representation. This feed-forward refinement enhances nonlinear feature transformation and improves the overall trajectory modeling accuracy.

## 4.6 Self-supervised Training

**Contrastive Loss.** To learn effective cross-modal representations between prompt-enhanced grid embedding and road network modalities, we employ a contrastive framework [21] that encourages alignment between semantically corresponding trajectory representations. Given a batch of trajectory pairs, where each sample contains both prompt-enhanced grid embedding visual representation and road network sequence representation, we aim to learn a shared embedding space where corresponding modalities are pulled together while non-corresponding pairs are pushed apart.

The contrastive learning objective employs InfoNCE loss with temperature scaling:

$$\mathcal{L}_{CL} = \frac{1}{2} [\mathcal{L}_{\tilde{G} \rightarrow R} + \mathcal{L}_{R \rightarrow \tilde{G}}], \quad (18)$$

where

$$\mathcal{L}_{\tilde{G} \rightarrow R} = -\frac{1}{N} \sum_{i=1}^N \log \frac{\exp(\tilde{G}_i \cdot R_i / \tau)}{\sum_{j=1}^N \exp(\tilde{G}_i \cdot R_j / \tau)}, \quad (19)$$

$$\mathcal{L}_{R \rightarrow \tilde{G}} = -\frac{1}{N} \sum_{i=1}^N \log \frac{\exp(R_i \cdot \tilde{G}_i / \tau)}{\sum_{j=1}^N \exp(R_i \cdot \tilde{G}_j / \tau)}. \quad (20)$$

Here,  $\tau$  is a learnable temperature parameter that controls the concentration of the distribution, and  $N$  is the batch size. The bidirectional formulation ensures symmetric learning between both modalities.

**Masked Language Modeling Loss (MLM Loss).** To capture sequential dependencies and contextual relationships in road network trajectories, we adopt a BERT-style masked language modeling strategy [5]. In each trajectory sequence, 15% of the road segments are randomly masked, and the model is trained to recover the original road IDs based on surrounding context and cross-modal information from the *prompt-enhanced grid representations*. This design encourages the model to jointly leverage contextual and cross-modal cues while mitigating overfitting to the [MASK] token.

For a masked road trajectory  $\tilde{s} = [s_1, s_2, \dots, [\text{MASK}], \dots, s_L]$ , the model predicts the original road segment IDs at the masked positions. The training objective is defined as:

$$\mathcal{L}_{\text{MLM}} = -\frac{1}{|M|} \sum_{i \in M} \log P(s_i | \tilde{s}, \tilde{G}, R), \quad (21)$$

where  $M$  denotes the set of masked positions, and  $P(s_i | \tilde{s}, \tilde{G}, R)$  represents the probability of correctly predicting the road segment  $s_i$  given the masked sequence  $\tilde{s}$  and its corresponding *prompt-enhanced grid context*.

This objective enables the model to learn rich contextual representations of road networks while leveraging spatial semantics from the prompt-enhanced grid modality, facilitating a deeper understanding of trajectory patterns and spatial dependencies.

**Joint Training Objective.** The final objective is the sum of the two self-supervised tasks:

$$\mathcal{L}_{\text{total}} = \mathcal{L}_{\text{CL}} + \mathcal{L}_{\text{MLM}}. \quad (22)$$

Both losses contribute equally, enabling the model to learn cross-modal alignment and intra-modal sequential patterns simultaneously.

## 5 Experiments

### 5.1 Experiment Settings

We evaluate the performance of MDTI on three real-world datasets. The experiments are designed to address the following research questions:

- **RQ1:** Does MDTI provide more accurate estimates of travel time compared to various baseline methods?
- **RQ2:** How do different components of the MDTI model contribute to the overall performance?
- **RQ3:** Can the dynamic trajectory modeling module of MDTI adapt to inputs of different trajectory lengths?
- **RQ4:** How is the transferability of MDTI?

Due to space limitations, we have placed RQ4 in the Appendices.

**Datasets.** We evaluate the proposed approach on three real-world multi-modal trajectory datasets collected from Porto, Chengdu, and Xi'an. Each dataset comprises GPS trajectories, route trajectories, and corresponding road networks. The GPS data are sourced from publicly available datasets released by Didi Chuxing<sup>1</sup>, while the road networks are extracted using OSMNX [2], which provides rich attributes such as road type, length, lane count, and topological connectivity. For model training, we utilize only the topological structure of the road networks, differing from some baseline configurations that incorporate additional road attributes. The raw GPS trajectories are map-matched to the corresponding road networks through a standard map-matching algorithm, resulting in route trajectories and an assignment matrix. The assignment matrix explicitly encodes the mapping between trajectory sub-segments and their associated road segments. For data partitioning, all datasets follow a consistent split across cities: 60% for training, 20% for validation, and 20% for testing.

**Implementation Details.** The proposed **MDTI** model integrates a GPS encoder, a grid encoder, a road encoder, a dynamic

trajectory alignment module, and a cross-modal interaction module, trained in an end-to-end manner. Training is performed with a batch size of 32 for 30 epochs. We adopt Adam [11] as the optimizer with an initial learning rate of  $2 \times 10^{-4}$ , cosine annealing schedule, 10 warm-up epochs, a minimum learning rate of  $1 \times 10^{-6}$ , and weight decay of  $1 \times 10^{-4}$ . Both hidden and output embedding dimensions are fixed at 256 with a dropout rate of 0.1. For GPS trajectories, each sequence is segmented into patterns and compared with historical keys, and the most relevant ones are transformed into natural language prompts. These prompts are encoded by a pre-trained GPT-2 model, where the hidden state of the last token is taken as the trajectory embedding. Grid and road representations are generated by Transformer and GAT layers, while the cross-modal module aligns multi-source features. The objective combines multiple loss terms with weights of relation=0.5, step=1.0, rel=1.0, and cos=1.0.

**Evaluation Metrics.** We adopt three widely-used regression metrics: Mean Absolute Error (MAE) for measuring average prediction error magnitude, Mean Absolute Percentage Error (MAPE) for assessing relative error percentage. These metrics collectively provide a comprehensive assessment of prediction accuracy and model robustness.

**Baselines.** We compare the proposed MDTI model with eight baseline methods, which can be categorized into four groups. All methods are trained using the same number of trajectories. The four groups include: one method based on GPS trajectories (e.g., Traj2vec [31]); one method based on grid trajectories (e.g., TrajCL [3]); four methods based on road trajectories (e.g., JCLRNT [20], START [10], JGRM [18], GREEN [33]); and two methods related to travel time estimation (e.g., DutyTTE [19] and Mult-TTE [15]). Further details about the baselines are provided in Appendices 7.1.

### 5.2 Performance Comparison (RQ1)

Table 1 presents the overall performance of our model and baseline methods across the three city datasets. Several key observations emerge: (1) Our method consistently achieves the best MAE on all datasets and the lowest MAPE on Chengdu and Xi'an. This confirms that the proposed cross-modal interaction module and modality-specific encoders within a unified feature space effectively enhance cross-domain alignment and semantic representation. In addition, the dynamic trajectory feature extraction mechanism adaptively balances information density across trajectories of varying lengths, mitigating local embedding bias. (2) Among single-modality trajectory modeling methods, Traj2vec—which directly encodes raw GPS point sequences—performs the worst, as RNN-based sequence modeling amplifies local noise. In contrast, TrajCL, which relies solely on grid representations, suffers from spatial discretization errors and the loss of fine-grained positional information. Road-network-based methods generally outperform both, indicating that the topological connectivity of road segments and intersections provides strong structural constraints, while road semantics and traffic rules capture more stable spatiotemporal patterns. (3) On the Porto dataset, our method performs slightly worse than Mult-TTE in terms of MAPE, likely due to MAPE's sensitivity to relative errors. Nevertheless, our approach achieves the lowest MAE, demonstrating superior robustness to outliers and measurement

<sup>1</sup><https://outreach.didichuxing.com/>

**Table 1: Performance comparison across three datasets. The best results are in bold and the second-best are underlined. ↓ means lower is better. Statistical significance was tested using paired t-tests across datasets; the differences were significant with  $p < 0.05$ .**

Method	Porto		Xi'an		Chengdu	
	MAE↓	MAPE↓	MAE↓	MAPE↓	MAE↓	MAPE↓
<b>GPS-based trajectory representation learning</b>						
Traj2vec	4.027	0.534	1.651	0.352	2.481	0.267
<b>Grid-based trajectory representation learning</b>						
TrajCL	2.085	0.236	1.632	0.321	1.609	0.536
<b>Travel Time Estimation Models</b>						
DutyTTE	3.780	0.303	4.131	0.302	4.525	0.316
MULT-TTE	1.524	<b>0.147</b>	<u>1.231</u>	<u>0.172</u>	1.461	0.234
<b>Road-based trajectory representation learning</b>						
START	1.541	0.173	1.764	0.282	1.359	0.218
JCLRNT	3.065	0.327	1.638	0.272	1.352	0.241
JGRM	2.993	0.375	1.457	0.333	1.374	0.360
GREEN	<u>1.510</u>	0.165	1.241	0.184	<u>1.322</u>	<u>0.185</u>
MDTI	<b>1.419</b>	0.152	<b>1.169</b>	<b>0.170</b>	<b>1.143</b>	<b>0.183</b>

noise. DutyTTE shows the weakest overall performance, as it lacks multimodal alignment and focuses primarily on global path consistency and interval coverage. (4) Overall, cross-modal trajectory representation learning methods outperform single-modality ones, confirming that multimodal information effectively compensates for modality-specific limitations. Furthermore, our dynamic fusion mechanism adaptively regulates information density according to trajectory length, preventing feature over-concentration in local segments. This design yields consistently stable performance across both short and long trajectories while reducing the impact of extreme values.

### 5.3 Component Contribution (RQ2)

**Ablation Settings.** To assess the contribution of each MDTI module, we conduct four ablations:

- **w/o GPS Enc.** Removes the GPS modality and the associated large language model, retaining only the road network and grid representations.
- **w/o Road Enc.** Removes the road network encoder, leaving only the GPS and grid encoders.
- **w/o Grid Enc.** Removes the grid modality; the embeddings generated by the GPS encoder are fused directly with the road network features.
- **w/o Dynamic Fusion** This variant removes the prompt-based Dynamic Fusion mechanism.

The outcomes of the ablation study conducted on the Porto dataset, as reported in Table 2, quantitatively validate the contribution of each component within the **MDTI** framework. Additional analyses and extended ablation results are provided in the Appendices 7.2.

**Importance of Multimodal Encoders.** Removing any single modality encoder results in a consistent performance decline across

all evaluation metrics (MAE and MAPE), highlighting the necessity of multimodal information fusion. Notably, the exclusion of the Grid Encoder yields the largest performance drop, indicating that grid-based spatial representations provide crucial contextual cues that complement the sequential dynamics captured by GPS trajectories and the topological structure encoded by the road network. The observed degradation when removing either the GPS Encoder or the Road Encoder further confirms that both trajectory dynamics and road topology contribute distinct and indispensable information for accurate TTE.

**Indispensability of the Dynamic Fusion Alignment Mechanism.** The experimental results clearly demonstrate that the proposed dynamic fusion alignment mechanism is crucial for maintaining the overall performance of the model. Its removal leads to a substantial drop across all evaluation metrics, producing outputs markedly inferior to those of the full model that benefits from dynamic feature alignment. Although some global metrics may appear comparable, qualitative inspection reveals evident spatial distortions and implausible artifacts in the predicted distributions. These findings confirm that the primary contribution of the dynamic fusion alignment mechanism lies in its ability to intelligently align and integrate multi-source features, ensuring spatial coherence and physical plausibility in model predictions, rather than merely optimizing global numerical accuracy.

**Table 2: Ablation study of different modules.**

	MAE↓	MAPE↓
w/o GPS enc.	1.441	0.153
w/o Road enc.	1.468	0.156
w/o Grid enc.	1.593	0.180
w/o Dynamic FusionAlign	1.457	0.154
<b>MDTI</b>	<b>1.419</b>	<b>0.152</b>

### 5.4 Trajectory Length Impact (RQ3)

We analyze the effect of fixed and dynamic trajectory lengths on model performance by comparing prediction error metrics. Specifically, we evaluate three fixed lengths (10, 65, and 120) and one dynamic adjustment strategy, using MAE, RMSE, and MAPE as evaluation metrics. The results are presented in Figure 3.

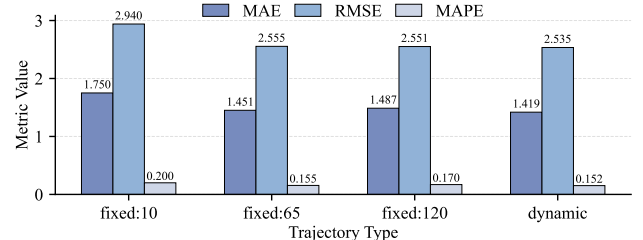


**Figure 3: Comparison of fixed and dynamic trajectory lengths on prediction errors.**

Under fixed-length conditions, prediction errors decrease as trajectory length increases. This phenomenon indicates that longer trajectories contain a more extensive history of object motion, thereby providing the model with more comprehensive information on

motion patterns. In contrast, shorter trajectories provide limited information, making it difficult for the model to distinguish whether an object is moving at a constant speed, accelerating, or turning, which increases the uncertainty of prediction. Furthermore, longer trajectories demonstrate stronger noise resistance. Short trajectories are highly sensitive to measurement noise or transient irregular movements (e.g., obstacle avoidance), where even a single abnormal point can significantly disturb the judgment of the overall trend; meanwhile, longer trajectories, by virtue of incorporating more data points, can effectively smooth out random noise and allow the model to focus on stable and intrinsic motion trends.

More importantly, the dynamic trajectory strategy consistently outperforms all fixed-length configurations across all error metrics. This result demonstrates that adaptive adjustment of the trajectory length allows the model to provide the most appropriate amount of contextual information for different motion scenarios, yielding optimal or near-optimal prediction performance.

## 6 CONCLUSION

This paper proposes a multimodal dynamic trajectory representation framework, **MDTI**, which integrates GPS sequences, grid trajectories, and road network constraints to learn diverse trajectory representations. Corresponding encoders are designed for these three types of trajectories. In addition, to address the limitations of fixed-length feature vectors, a dynamic fusion module is developed. Finally, two loss functions are designed to enhance the framework's performance. Experiments on three datasets demonstrate that MDTI outperforms state-of-the-art baseline methods.

## References

- Ove Andersen and Kristian Torp. 2017. Sampling frequency effects on trajectory routes and road network travel time. In *Proceedings of the 25th ACM SIGSPATIAL International Conference on Advances in Geographic Information Systems*. 1–10.
- Geoff Boeing. 2017. OSMnx: New methods for acquiring, constructing, analyzing, and visualizing complex street networks. *Computers, environment and urban systems* 65 (2017), 126–139.
- Yanchuan Chang, Jianzhong Qi, Yuxuan Liang, and Egemen Tanin. 2023. Contrastive Trajectory Similarity Learning with Dual-Feature Attention. arXiv:2210.05155 [cs.DB] <https://arxiv.org/abs/2210.05155>
- Zebin Chen, Xiaolin Xiao, Yue-Jiao Gong, Jun Fang, Nan Ma, Hua Chai, and Zhiqiang Cao. 2022. Interpreting trajectories from multiple views: A hierarchical self-attention network for estimating the time of arrival. In *Proceedings of the 28th ACM SIGKDD Conference on Knowledge Discovery and Data Mining*. 2771–2779.
- Jacob Devlin, Ming-Wei Chang, Kenton Lee, and Kristina Toutanova. 2019. Bert: Pre-training of deep bidirectional transformers for language understanding. In *Proceedings of the 2019 conference of the North American chapter of the association for computational linguistics: human language technologies, volume 1 (long and short papers)*. 4171–4186.
- Ziqian Fang, Yuntao Du, Lu Chen, Yujia Hu, Yunjun Gao, and Gang Chen. 2021. E2DTC: An End to End Deep Trajectory Clustering Framework via Self-Training. In *2021 IEEE 37th International Conference on Data Engineering (ICDE)*. 696–707. doi:10.1109/ICDE51399.2021.00066
- Tao-Yang Fu and Wang-Chien Lee. 2020. Trembr: Exploring road networks for trajectory representation learning. *ACM Transactions on Intelligent Systems and Technology (TIST)* 11, 1 (2020), 1–25.
- Jindong Han, Hao Liu, Shui Liu, Xi Chen, Naiqiang Tan, Hua Chai, and Hui Xiong. 2023. iETA: A robust and scalable incremental learning framework for time-of-arrival estimation. In *Proceedings of the 29th ACM SIGKDD Conference on Knowledge Discovery and Data Mining*. 4100–4111.
- Sepp Hochreiter and Jürgen Schmidhuber. 1997. Long short-term memory. *Neural computation* 9, 8 (1997), 1735–1780.
- Jiawei Jiang, Dayan Pan, Houxiang Ren, Xiaohan Jiang, Chao Li, and Jingyuan Wang. 2023. Self-supervised trajectory representation learning with temporal regularities and travel semantics. In *2023 IEEE 39th international conference on data engineering (ICDE)*. IEEE, 843–855.
- Diederik P Kingma. 2014. Adam: A method for stochastic optimization. arXiv preprint arXiv:1412.6980 (2014).
- Xiucheng Li, Kaiqi Zhao, Gao Cong, Christian S Jensen, and Wei Wei. 2018. Deep representation learning for trajectory similarity computation. In *2018 IEEE 34th international conference on data engineering (ICDE)*. IEEE, 617–628.
- Xiucheng Li, Kaiqi Zhao, Gao Cong, Christian S Jensen, and Wei Wei. 2018. Deep Representation Learning for Trajectory Similarity Computation. In *2018 IEEE 34th International Conference on Data Engineering (ICDE)*. 617–628. doi:10.1109/ICDE.2018.00062
- Yaguang Li, Kun Fu, Zheng Wang, Cyrus Shahabi, Jieping Ye, and Yan Liu. 2018. Multi-task representation learning for travel time estimation. In *Proceedings of the 24th ACM SIGKDD international conference on knowledge discovery & data mining*. 1695–1704.
- Tianxi Liao, Liangzhe Han, Yi Xu, Tongyu Zhu, Leilei Sun, and Bowen Du. 2024. Multi-faceted route representation learning for travel time estimation. *IEEE Transactions on Intelligent Transportation Systems* 25, 9 (2024), 11782–11793.
- Hao Liu, Wenzhao Jiang, Shui Liu, and Xi Chen. 2023. Uncertainty-aware probabilistic travel time prediction for on-demand ride-hailing at didi. In *Proceedings of the 29th ACM SIGKDD Conference on Knowledge Discovery and Data Mining*. 4516–4526.
- Yin Lou, Chengyang Zhang, Yu Zheng, Xing Xie, Wei Wang, and Yan Huang. 2009. Map-matching for low-sampling-rate GPS trajectories. In *Proceedings of the 17th ACM SIGSPATIAL international conference on advances in geographic information systems*. 352–361.
- Zhipeng Ma, Zheyuan Tu, Xinhai Chen, Yan Zhang, Deguo Xia, Guyue Zhou, Yilun Chen, Yu Zheng, and Jianguo Gong. 2024. More than routing: Joint GPS and route modeling for refine trajectory representation learning. In *Proceedings of the ACM Web Conference 2024*. 3064–3075.
- Xiaowei Mao, Yan Lin, Shengnan Guo, Yubin Chen, Xingyu Xian, Haomin Wen, Qisen Xu, Youfang Lin, and Huaiyu Wan. 2025. DutyTTE: Deciphering Uncertainty in Origin-Destination Travel Time Estimation. In *Proceedings of the AAAI Conference on Artificial Intelligence*, Vol. 39. 12390–12398.
- Zhenyu Mao, Ziyue Li, Dedong Li, Lei Bai, and Rui Zhao. 2022. Jointly contrastive representation learning on road network and trajectory. In *Proceedings of the 31st ACM International Conference on Information & Knowledge Management*. 1501–1510.
- Alec Radford, Jong Wook Kim, Chris Hallacy, Aditya Ramesh, Gabriel Goh, Sandhini Agarwal, Girish Sastry, Amanda Askell, Pamela Mishkin, Jack Clark, et al. 2021. Learning transferable visual models from natural language supervision. In *International conference on machine learning*. PMLR, 8748–8763.

- [22] Royston Rodrigues, Neha Bhargava, Rajbabu Velmurugan, and Subhasis Chaudhuri. 2020. Multi-timescale trajectory prediction for abnormal human activity detection. In *Proceedings of the IEEE/CVF winter conference on applications of computer vision*. 2626–2634.
- [23] Ilya Sutskever, Oriol Vinyals, and Quoc V Le. 2014. Sequence to sequence learning with neural networks. *Advances in neural information processing systems* 27 (2014).
- [24] Ashish Vaswani, Noam Shazeer, Niki Parmar, Jakob Uszkoreit, Llion Jones, Aidan N Gomez, Łukasz Kaiser, and Illia Polosukhin. 2017. Attention is all you need. *Advances in neural information processing systems* 30 (2017).
- [25] Petar Veličković, Guillem Cucurull, Arantxa Casanova, Adriana Romero, Pietro Lio, and Yoshua Bengio. 2017. Graph attention networks. *arXiv preprint arXiv:1710.10903* (2017).
- [26] Dong Wang, Junbo Zhang, Wei Cao, Jian Li, and Yu Zheng. 2018. When will you arrive? Estimating travel time based on deep neural networks. In *Proceedings of the AAAI conference on artificial intelligence*, Vol. 32.
- [27] Guo-Wei Wang, Jin-Dou Zhang, and Jing Li. 2018. Complete your mobility: Linking trajectories across heterogeneous mobility data sources. *Journal of Computer Science and Technology* 33, 4 (2018), 792–806.
- [28] Hongjian Wang, Xianfeng Tang, Yu-Hsuan Kuo, Daniel Kifer, and Zhenhui Li. 2019. A simple baseline for travel time estimation using large-scale trip data. *ACM Transactions on Intelligent Systems and Technology (TIST)* 10, 2 (2019), 1–22.
- [29] Can Yang and Gyozo Gidofalvi. 2018. Fast map matching, an algorithm integrating hidden Markov model with precomputation. *International Journal of Geographical Information Science* 32, 3 (2018), 547–570.
- [30] Di Yao, Haonan Hu, Lun Du, Gao Cong, Shi Han, and Jingping Bi. 2022. Trajgat: A graph-based long-term dependency modeling approach for trajectory similarity computation. In *Proceedings of the 28th ACM SIGKDD conference on knowledge discovery and data mining*. 2275–2285.
- [31] Di Yao, Chao Zhang, Zhihua Zhu, Jianhui Huang, and Jingping Bi. 2017. Trajectory clustering via deep representation learning. In *2017 international joint conference on neural networks (IJCNN)*. IEEE, 3880–3887.
- [32] Shuochao Yao, Shaohan Hu, Yiran Zhao, Aston Zhang, and Tarek Abdelzaher. 2017. Deepsense: A unified deep learning framework for time-series mobile sensing data processing. In *Proceedings of the 26th international conference on world wide web*. 351–360.
- [33] Silin Zhou, Shuo Shang, Lisi Chen, Peng Han, and Christian S Jensen. 2025. Grid and road expressions are complementary for trajectory representation learning. In *Proceedings of the 31st ACM SIGKDD Conference on Knowledge Discovery and Data Mining* V. 1. 2135–2146.

## 7 APPENDICES

### 7.1 Baseline

#### 1. GPS-based trajectory representation learning.

- **Traj2vec** [31]: An RNN-based seq2seq model converts GPS trajectory into feature sequence to learn trajectory representations.

#### 2. Grid-based trajectory representation learning.

- **TrajCL** [3]: The state-of-the-art grid-based method proposes a set of trajectory augmentations on grid trajectory in free space and dual-feature self-attention to learn grid trajectory representations using contrastive learning with the Transformer.

#### 3. Road-based trajectory representation learning.

- **JCLRNT** [20]: A jointly contrastive learning framework that performs within-road, within-trajectory, and cross-scale road-trajectory contrast, maximizing mutual information to obtain robust representations.
- **START** [10]: A self-supervised trajectory representation model that incorporates temporal regularities and travel semantics using a graph attention network and a time-aware trajectory encoder, trained with span-masked recovery and contrastive learning tasks.
- **JGRM** [18]: A joint GPS–route modeling approach with dual encoders and a cross-modal interaction module, trained in a self-supervised manner via masked language modeling (MLM) and cross-modal matching (CMM) objectives.

- **GREEN** [33]: A multimodal trajectory representation method that jointly leverages grid-based and road-based trajectories, aligned and fused via contrastive learning and masked reconstruction objectives.

### 4. Travel Time Estimation Models.

- **DutyTTE** [19]: A reinforcement learning-based framework that enhances the alignment between predicted and actual travel routes, and employs a mixture-of-experts mechanism to quantify uncertainty across different road segments.
- **MuLT-TTE** [15]: A multi-faceted model that decomposes routes into trajectory, attribute, and semantic sequences, combines sequential learning with Transformer encoders, and incorporates self-supervised masking and multi-task optimization.

**Table 3: Ablation study of loss components.**

	MAE $\downarrow$	MAPE $\downarrow$
w/o CL loss	1.418	<b>0.151</b>
w/o MLM loss	1.540	0.167
<b>MDTI</b>	<b>1.419</b>	0.152

**Table 4: The transferability accuracy of MDTI across three cities.**

Scenario	MAE $\downarrow$	RMSE $\downarrow$	MAPE $\downarrow$
Porto $\rightarrow$ Chengdu			
w/ Transfer	1.157	1.634	0.193
w/o Transfer	1.144	1.508	0.184
Chengdu $\rightarrow$ Xi'an			
w/ Transfer	1.153	1.568	0.173
w/o Transfer	1.169	1.614	0.170

### 7.2 Additional Ablation Studies

In Table 3, we further include two additional ablation experiments that examine the effects of removing the MLM loss and the CL loss, respectively.

Ablating the two self-supervised loss components further validates their essential roles in the model. Removing the MLM loss results in a more substantial performance drop than removing the CL loss, indicating that the MLM objective—which reconstructs masked road segments using contextual and grid information—plays a crucial role in capturing intra-modal dependencies and enhancing spatial–temporal representations. In contrast, the smaller degradation observed when excluding the CL loss suggests that, although cross-modal alignment is weakened, the model can still learn meaningful embeddings through the MLM objective and supervised optimization. Nevertheless, the best performance is achieved when both loss functions are jointly optimized, confirming their complementary contributions to improving representation quality and downstream travel time estimation accuracy.

### 7.3 Transferability Study (RQ4)

In Table 4, we evaluate the transferability of our pre-trained model across distinct urban scenarios through a series of experiments. In particular, we fine-tuned the model on the TTE task to adapt it to different city environments, while employing the transferred prompt files during task training.

The results demonstrate that transferring from Porto to Chengdu did not yield additional improvements; instead, the performance slightly declined. Nevertheless, the outcomes remain competitive compared with other baselines. This phenomenon may be attributed to the substantial differences in traffic patterns between the two

cities, which limit the effectiveness of transfer learning. Conversely, transferring from Chengdu to Xi'an led to overall performance gains, suggesting that the two cities share more similar traffic characteristics, thereby enabling transfer learning to exert a positive effect.